

Received May 7, 2019, accepted June 5, 2019, date of publication June 10, 2019, date of current version July 1, 2019.

Digital Object Identifier 10.1109/ACCESS.2019.2921808

# Study of Propagation Channel Characteristics for Underwater Acoustic Communication Environments

JIE ZHOU<sup>1,2</sup>, (Senior Member, IEEE), HAO JIANG<sup>1</sup>, (Member, IEEE), PENG WU<sup>1</sup>, AND QIAN CHEN<sup>1</sup>

<sup>1</sup>College of Electronic and Information Engineering, Nanjing University of Information Science and Technology, Nanjing 210044, China

<sup>2</sup>College of Electronic and Electrical Engineering, Niigata University, Niigata 950-2181, Japan

Corresponding author: Hao Jiang (jianghao@nuist.edu.cn)

This work was supported in part by the National Natural Science Foundation of China under Grant 61771248, in part by the Major Program of the Natural Science Foundation of Institution of Higher Education of Jiangsu Province under Grant 14KJA510001, in part by the Startup Foundation for Introducing Talent of NUIST, and in part by the Priority Academic Program Development of Jiangsu Higher Education Institutions.

**ABSTRACT** For the study of propagation characteristics in underwater acoustic channels, a geometry-based model is introduced to represent the multipath scattering environments between a transmitter (Tx) and a mobile receiver (MR). To consider the impact of the scattering environments on the propagation characteristics with low complexity, we adopt a rectangle to describe the communication environments of the vertical cross section of the ocean, where the scatterers are assumed to be randomly distributed on the surface and bottom of the sea. In the model, we first derive the closed-form expressions for the probability density functions (PDFs) of the angle of departure (AoD) and angle of arrival (AoA) statistics. Then, we investigate the spatial and frequency correlation functions of two different propagation paths. The numerical simulation results fit the conventional results very well, which demonstrate that the proposed model has the ability to describe the underwater acoustic communication environments.

**INDEX TERMS** Underwater acoustic channels, geometry-based channel model, angle of departure AoD and angle of arrival AoA statistics, spatial and frequency correlation functions.

## I. INTRODUCTION

### A. MOTIVATION

Underwater wireless networks, which have the advantages of scientific exploration, tactical surveillance, and offshore exploration, have been widely researched in wireless communication systems [1]. To make these applications feasible, it is important to design and analyse wireless underwater acoustic communication systems. In light of this, statistical propagation characteristics of underwater communication channel are necessary to assess system performance to improve the quality of a communication system [2].

### B. RELATED WORKS

The existing literatures have done a variety of studies on the simulation of underwater acoustic wireless channels, which are usually based on the experimental data obtained in some

actual communication scenarios. Kebkal *et al* [3] developed experimental results of implementing network coding in real underwater acoustic environments, which demonstrated a significant improvement of network performance with network coding versus the standard queuing approach. It is worth mentioning that, the distribution of scatterers determines the statistical characteristics, e.g., angle of departure (AoD) and angle of arrival (AoA). Therefore, it is essential to introduce geometry-based channel models to describe the scatter distributions in underwater acoustic communication environments. In light of this, the closed-form expressions of the propagation characteristics are of great importance to the estimation of physical parameters such as AoD and AoA statistics [4].

As demonstrated in [5], the underwater acoustic propagation is characterized by attenuation that increases with signal frequency, time-varying multipath propagation, and low speed of sound. In reality, the existing studies have proposed a variety of multi-input multi-output (MIMO) multipath fading

The associate editor coordinating the review of this manuscript and approving it for publication was Guan Gui.

channels for underwater communication environments. To be specific, Jia *et al.* [6] proposed a wide-sense stationary uncorrelated scattering (WSSUS) channel model to characterize the shallow underwater acoustic channel propagation properties, which had a very important practical significance for the evaluation of system performance. In [7] and [8], we proposed geometric MIMO channel models for mobile radio communication environments, which assumed that the waves from the transmitter to the receiver experienced the line-of-sight (LoS) and non-LoS (NLoS) propagation rays. Abdi and Guo [9] were the first to investigate the frequency correlation functions for the time-invariant stationary underwater channels. Zajic [10] and [11] proposed geometry-based statistical models for wideband MIMO mobile-to-mobile (M2M) underwater multipath fading channels, which investigated the time and frequency correlation functions of two different propagation paths in shallow-water isovelocity communication environments.

In general, the isovelocity assumption does not hold in many real-world communication scenarios. Therefore, Naderi *et al.* [12] developed geometric channel models to reflect the non-isovelocity underwater acoustic propagation environments. Furthermore, Wang *et al.* [13] focused on the characterizing underwater acoustic channels in the view of wireless cognitive networks, which studied the unique propagation characteristics in underwater acoustic environments. In addition, Yang [14] measured an optimal output symbol signal noise ratio (SNR) for various subarrays with different receiver separations and aperture lengths in underwater acoustic communications. However, in reality, for the above geometry-based channel models in underwater acoustic environments, the AoA and AoD statistics caused by the waves scattered from the surface and bottom of the sea have not been derived. Meanwhile, the spatial correlation function of different propagation rays scattered from the surface and bottom of the sea are not investigated. Therefore, these models cannot realistically describe the underwater acoustic communication environments.

### C. MAIN CONTRIBUTIONS

In this paper, we propose a geometry-based channel model for underwater acoustic communication environments, which assume that the scatterers are randomly distributed on the surface and bottom of the sea, as illustrated in Fig. 1. The proposed model is the combination of LoS components, NLoS rays scattered by the scatterers on the surface of the sea, and NLoS rays scattered by the scatterers on the bottom of the sea. In this paper, we first derive the closed-form expressions for the probability density functions (PDFs) of the AoA and AoD statistics. Then, we investigate the spatial and frequency correlation functions of two different propagation paths. From numerical results and observations, the main contributions of this paper are shown as follows: (1) The proposed underwater acoustic channel model can be used to simulate a variety of wireless communication environments. (2) We introduce the equally spaced scatterers to describe

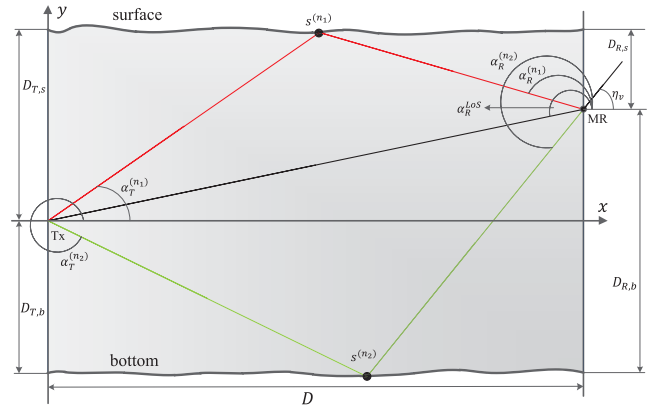


FIGURE 1. Illusion of the geometric path lengths and geometric angles in the proposed underwater acoustic channel model.

the proposed simulation model for underwater acoustic environments. Numerical results demonstrate that the proposed underwater acoustic channel model with MESS method has the ability to provide the system with better performance than the traditional Lp-norm method.

The remainder of this paper is organized as follows. Section II presents the proposed system channel model for underwater acoustic communication environments. In Section III, the theoretical propagation properties of the channel model are derived and investigated. Section IV provides the numerical results and discussions. Finally, our conclusions are presented in Section V.

## II. SYSTEM CHANNEL MODEL

Figure 1 shows a typical underwater acoustic communication scenario with LoS and NLoS propagation rays, where the transmitter (Tx) and mobile receiver (MR) are equipped with omnidirectional antenna arrays. The proposed model employs a geometric approach to represent the multipath propagation channel between a Tx and a MR. To consider the impact of the underwater scattering environments on the propagation characteristics, we adopt a rectangle to describe the scattering environments of the vertical cross section of the ocean, where the scatterers are assumed to be randomly distributed on the surface and bottom of the sea. Similar assumption can be seen in [10]. Let us define the line connecting the Tx and the MR along the bottom of the sea as the  $x$ -axis. The distance from the Tx to the MR along the  $x$ -axis is denoted as  $D_0$ . The distances from the Tx to the surface and bottom of the sea are denoted as  $D_{T,s}$  and  $D_{T,b}$ , respectively. Similarly, the distances from the MR to the surface and bottom of the sea are denoted as  $D_{R,s}$  and  $D_{R,b}$ , respectively. In the model, the Tx is fixed while the MR is in motion; thus, the moving direction and velocity of the MR are denoted as  $\eta_v$  and  $v_R$ , respectively. It is assumed that there are  $N_1$  effective scatterers existing on the surface of the sea, and the  $n_1$ -th ( $n_1 = 1, \dots, N_1$ ) object is defined as  $s^{(n_1)}$ .  $N_2$  effective scatterers likewise exist on the bottom of the sea, and the  $n_2$ -th ( $n_2 = 1, \dots, N_2$ ) object is defined

as  $s^{(n_2)}$ . The AoDs of the transmit propagation paths related to the surface and bottom of the sea are denoted as  $\alpha_T^{(n_1)}$  and  $\alpha_T^{(n_2)}$ , respectively. The AoAs of the receive propagation paths related to the surface and bottom of the sea are denoted as  $\alpha_R^{(n_1)}$  and  $\alpha_R^{(n_2)}$ , respectively. Furthermore, the AoA of the LoS component is denoted as  $\alpha_R^{LoS}$ .

### III. CHANNEL COMPLEX IMPULSE RESPONSE

In general, MIMO fading channel models can be characterized by an matrix, which is composed of a series of channel complex impulse response. It has been reported in [15] that the complex gain information and AoD/AoA information are two key characteristics of the channel matrix. To achieve super-resolution channel estimation, the authors in [16] and [17] introduced the deep learning based framework to obtain the physical AoD/AoA information, which was incorporated into the complex gain information to realize the channel estimation. However, in the proposed single-input single-output (SISO) channel model, the physical properties can be described by the channel complex impulse response. Note that the received signals are composed of the LoS rays, NLoS rays scattered from the surface of the sea, and NLoS rays scattered from the bottom of the sea, as shown in Fig. 1. Therefore, the channel complex impulse response of the proposed model can be expressed as

$$h(t, \tau') = h_0(t, \tau') + \sum_{\ell=0}^2 h_\ell(t, \tau') \quad (1)$$

In (1), the channel impulse response of the LoS component  $h_0(t, \tau')$  can be expressed as

$$h_0(t, \tau') = \sqrt{\frac{K}{1+K}} A_s(D_0) A_a(D_0) \times e^{j(2\pi f_0 t + \varphi_0)} \delta(\tau' - \tau'_0) \quad (2)$$

where  $K$  denotes the rice factor,  $\tau'_0$  is the propagation delay of the LoS component. It is assumed that the initial phase  $\varphi_0$  is an independent random variable, which has a uniform distribution in the interval from  $-\pi$  to  $\pi$ , i.e.,  $\varphi_0 \sim [-\pi, \pi)$ . The Doppler frequency  $f_0$  of the LoS component can be expressed as

$$f_0 = \frac{v_R}{c_s} \cos(\alpha_R^{LoS} - \eta_v) \quad (3)$$

where  $c_s$  denotes the speed of the sound propagation in the sea, i.e.,  $c_s = 1500$  m/s (isokinetic environment). Observe from the geometrical model parameters in Fig. 1, the AoA  $\alpha_R^{LoS}$  and propagation delay  $\tau'_0$  can be respectively expressed as

$$\alpha_R^{LoS} = \pi + \arctan\left(\frac{D_{T,s} - D_{R,s}}{D_0}\right) \quad (4)$$

$$\tau'_0 = \frac{1}{c_s} \sqrt{D_0^2 + (D_{T,s} - D_{R,s})^2} \quad (5)$$

It is worth mentioning that the  $A_s(D_0)$  and  $A_a(D_0)$  represent the coefficients of the path loss caused by the spherical

distribution and energy absorption, respectively, which can be expressed as [18]

$$A_s(D_0) = 1/D_0 \quad (6)$$

$$A_a(D_0) = 10^{-\frac{1}{20000} \times D_0^\kappa} \quad (7)$$

It has been reported in [19] that, the carrier frequency in underwater acoustic wireless communication environments can be approximately defined between 3 ~ 100 kHz. Then, the expression of the parameter  $\kappa$  can be derived as

$$\kappa = 8.68 \times 10^3 \times (1 - 6.54 \times 10^{-4} P) \times \left( \frac{S_a f_T f_c^2 A}{f_c^2 + f_T^2} + \frac{B f_c^2}{f_T} \right) \quad (8)$$

where

$$A = 2.34 \times 10^{-6},$$

$$B = 3.36 \times 10^{-6},$$

$$P = 1.01(1 + 0.1 D_h),$$

the  $S_a$  denotes the salt content of the water in the sea,  $f_c$  is the carrier frequency,  $T$  is the temperature,  $D_h$  is the depth. In wireless channels, it is necessary to consider the LoS and NLoS between a Tx and a MR [20]. It is worth mentioning that in underwater acoustic communication environments, the LoS component is usually blocked by obstacles in complicated environments, and therefore, the LoS component is very weak, while the NLoS components are dominant in the signal received at the MR. In the proposed model, the signal from the Tx impinges on the scatterers on the surface and bottom of the sea before reaching the MR. Therefore, when the waves from the Tx impinge on the scatterer  $s^{(n_\ell)}$  ( $\ell = 1, 2$ ) before reaching the MR, the channel impulse response can be expressed as

$$h_\ell(t, \tau') = \lim_{N_\ell \rightarrow \infty} \sum_{n_\ell=1}^{N_\ell} \frac{1}{\sqrt{2N_\ell(1+K)}} \times A_s(D_{n_\ell}) A_a(D_{n_\ell}) \times e^{j(2\pi f_{n_\ell} t + \varphi_0)} \delta(\tau' - \tau'_{n_\ell}) \quad (9)$$

where  $\tau'_{n_\ell}$  denotes the propagation delay of the  $\ell$ -th path,  $D_{n_\ell}$  is the propagation delay of the waves from the Tx impinge on the scatterer  $s^{(n_\ell)}$  before arriving at the MR, which can be expressed as

$$D_{n_\ell} = \frac{D_{T,s}}{\sin \alpha_T^{(n_\ell)}} + \frac{D_{R,s}}{\sin \alpha_R^{(n_\ell)}} \quad (10)$$

The Doppler frequency  $f_{n_\ell}$  of the NLoS component can be expressed as

$$f_{n_\ell} = \frac{v_R}{c_s} \cos(\alpha_R^{(n_\ell)} - \eta_v) \quad (11)$$

Based on the above model parameters, we further analyze the propagation characteristics of the proposed model in the following.

**A. PDFS OF THE AOD AND AOA STATISTICS**

In this section, we investigate the spatial characteristics of the AoA and AoD statistics of the proposed model. Let us assume that the scatterers are uniformly distributed on the surface and bottom of the sea. It is worth mentioning that when the number of scatterers tends to be infinity, the discrete random variables can be transformed into the continuous random variables. Therefore, the joint PDF of the scatter distribution can be expressed as

$$P_{xy}(x, y) = \begin{cases} \frac{1}{2D} [\delta(y - D_{T,s}) + \delta(y + D_{T,b})], & 0 \leq x \leq D_0 \\ 0, & \text{otherwise} \end{cases} \quad (12)$$

Note that the AoD  $\alpha_T^{(n_\ell)}$  has different closed-form expressions as the  $x$  varies, which can be expressed as

$$\alpha_T^{(n_\ell)} = \begin{cases} \arctan\left(\frac{D_{T,s}}{x}\right), & 0 \leq x \leq D_0 \\ \frac{3\pi}{2} + \arctan\left(\frac{x}{D_{T,b}}\right), & \text{otherwise} \end{cases} \quad (13)$$

Based on the principle of random variable transformation, the PDF of the AoD statistics can be expressed as

$$p(\alpha_T^{(n_\ell)}) = \begin{cases} \frac{D_{T,s}}{2D \sin^2 \alpha_T^{(n_\ell)}}, & \arctan\left(\frac{D_{T,s}}{D}\right) \leq \alpha_T^{(n_\ell)} \leq \frac{\pi}{2} \\ \frac{D_{T,b}}{2D \sin^2 \alpha_T^{(n_\ell)}}, & \frac{3\pi}{2} \leq \alpha_T^{(n_\ell)} \leq \arctan\left(\frac{D_{T,s}}{D}\right) \end{cases} \quad (14)$$

However, the AoA  $\alpha_R^{(n_\ell)}$  can be expressed as

$$\alpha_R^{(n_\ell)} = \begin{cases} \frac{\pi}{2} + \arctan\left(\frac{D_0 - x}{D_{R,s}}\right), & 0 \leq x \leq D_0 \\ \pi + \arctan\left(\frac{D_{R,b}}{D_0 - x}\right), & \text{otherwise} \end{cases} \quad (15)$$

It is worth mentioning that the PDF of the AoA statistics can be obtained by using the principle of random process conversion again, i.e.,

$$p(\alpha_R^{(n_\ell)}) = \begin{cases} \frac{D_{R,s}}{2D \sin^2 \alpha_R^{(n_\ell)}}, & \frac{\pi}{2} \leq \alpha_R^{(n_\ell)} \leq \arctan\left(\frac{D_0}{D_{R,s}}\right) \\ \frac{D_{R,b}}{2D \sin^2 \alpha_R^{(n_\ell)}}, & \pi + \arctan\left(\frac{D_{R,b}}{D_0}\right) \leq \alpha_R^{(n_\ell)} \leq \frac{3\pi}{2} \end{cases} \quad (16)$$

According to the geometric relationships between the AoD  $\alpha_T^{(n_\ell)}$  and AoA  $\alpha_R^{(n_\ell)}$ , we can obtain

$$\alpha_T^{(n_\ell)}(\alpha_R^{(n_\ell)}) = \begin{cases} \arctan\left(\frac{D_{R,s} \tan \alpha_R^{(n_\ell)}}{D_0 \tan \alpha_R^{(n_\ell)} + D_{R,s}}\right), & \frac{\pi}{2} \leq \alpha_R^{(n_\ell)} \leq \arctan\left(\frac{D_0}{D_{R,s}}\right) \\ \frac{3\pi}{2} + \arctan\left(\frac{D_0 \tan(\alpha_R^{(n_\ell)} - \pi) - D_{R,b}}{D_{T,b} \tan(\alpha_R^{(n_\ell)} - \pi)}\right), & \pi + \arctan\left(\frac{D_{R,b}}{D_0}\right) \leq \alpha_R^{(n_\ell)} \leq \frac{3\pi}{2} \end{cases} \quad (17)$$

It is worth mentioning that the AoD and AoA statistics of the multi-path components can be used to evaluate the performance of wireless communication systems [21]. Based on the above PDFs of the closed-form expressions of the AoD/AoA statistics, we investigate the spatial and frequency correlation functions of two different propagation paths in the following subsections.

**B. PROPAGATION DELAY**

In this subsection, the temporal statistics of the propagation delay in underwater acoustic channels are derived and discussed. Here,  $\tau'$  is the propagation delay of a multi-path signal reflected from any one scatterer on the surface and bottom of the sea in the proposed model. Therefore, the propagation delay of the  $\ell$ -th path can be expressed as

$$\tau'_{n_\ell} = \frac{D_{n_\ell}}{K} \quad (18)$$

In substituting (10) and (17) into (18), the propagation delay  $\tau'(\alpha_R^{(n_\ell)})$  can be expressed as

$$\tau'(\alpha_R^{(n_\ell)}) = \begin{cases} \frac{1}{K} \left( \frac{D_{T,s}}{\sin(\alpha_T^{(n_\ell)}(\alpha_R^{(n_\ell)}))} + \frac{D_{R,s}}{\sin \alpha_R^{(n_\ell)}} \right), & \frac{\pi}{2} \leq \alpha_R^{(n_\ell)} \leq \arctan\left(\frac{D}{D_{R,s}}\right) \\ \frac{1}{K} \left( \frac{D_{T,b}}{\sin(\alpha_T^{(n_\ell)}(\alpha_R^{(n_\ell)}))} + \frac{D_{R,b}}{\sin \alpha_R^{(n_\ell)}} \right), & \pi + \arctan\left(\frac{D_{R,b}}{D}\right) \leq \alpha_R^{(n_\ell)} \leq \frac{3\pi}{2} \end{cases} \quad (19)$$

**C. SPATIAL CORRELATION FUNCTION**

To calculate the spatial correlation of the proposed model, it is important to deduce the time-varying complex channel transfer function in advance. As demonstrated in [19], the channel complex impulse response can be obtained by Fourier transformation delay propagation of the complex channel transfer function, i.e.,

$$H(t, \tau') = H_0(t, \tau') + \sum_{\ell=0}^2 H_\ell(t, \tau') \quad (20)$$

where

$$H_0(t, \tau') = \sqrt{\frac{1}{K+1}} A_s(D_0) A_a(D_0) \times e^{j\varphi_0 + j2\pi(f_0 t - f'_0 \tau')} \quad (21)$$

$$H_\ell(t, \tau') = \lim_{N_\ell \rightarrow \infty} \sum_{n_\ell=1}^{N_\ell} \frac{1}{\sqrt{2N_\ell(1+K)}} \times A_s(D_{n_\ell}) A_a(D_{n_\ell}) \times e^{j\varphi_0 + j2\pi(f_{n_\ell} t - f'_{n_\ell} \tau'_{n_\ell})} \quad (22)$$

According to the central limit theorem, the time-varying complex channel transfer functions  $H_1(t, \tau')$  and  $H_2(t, \tau')$  are independent zero mean complex Gaussian processes, which can be calculated through the channel conversion function.



It is assumed that the underwater acoustic channel in the frequency and time domains are stationary. Therefore, the time-varying correlation function of two different propagation components can be expressed as

$$\rho_{HH}(\tau, \nu') = \frac{\mathbb{E}\{H(t, \nu')H^*(t + \tau, t + \nu')\}}{\mathbb{E}\{|H(t, \nu')|^2\}} \quad (23)$$

where  $(\cdot)^*$  denotes the complex conjugate process,  $\mathbb{E}\{\cdot\}$  is the statistical expectation factor applies to the random phase  $\varphi_0$ . The  $\nu'$  and  $\tau$  are the frequency and time interval variables, respectively. Therefore, the normalized spatial correlation function of two different LoS propagation components can be expressed as

$$\begin{aligned} \rho_{H_0 H_0}(\tau, \nu') &= \frac{\mathbb{E}\{H_0(t, \nu')H_0^*(t + \tau, t + \nu')\}}{A_s^2(D_0)A_a^2(D_0)} \\ &= \frac{K}{1 + K} e^{j2\pi\left[\frac{\nu_R}{c_s} \cos(\alpha_R^{LoS} - \eta_\nu)\tau - \nu'\tau'_0\right]} \end{aligned} \quad (24)$$

However, when the waves from the Tx impinge on the effective scatterers on the surface and bottom of the sea before arriving at the MR, the normalized spatial correlation function of two different propagation components can be derived as follows:

$$\begin{aligned} \rho_{H_\ell H_\ell}(\tau, \nu') &= \frac{1}{\chi_\ell(1 + K)} \\ &\times \int_{\alpha \in I_{\alpha, \ell}} e^{j2\pi\left[\frac{\nu_R}{c_s} \cos(\alpha_R^{(n_\ell)} - \eta_\nu)\tau_{n_\ell} - \nu'\tau'_{n_\ell}(\alpha_R^{(n_\ell)})\right]} \\ &\times A_s^2(D_{n_\ell}(\alpha_R^{(n_\ell)}))A_a^2(D_{n_\ell}(\alpha_R^{(n_\ell)})) \\ &p(\alpha_R^{(n_\ell)})d\alpha_R^{(n_\ell)} \end{aligned} \quad (25)$$

where  $\chi_\ell = \mathbb{E}\{A_s(D_{n_\ell}(\alpha_R^{(n_\ell)}))A_a(D_{n_\ell}(\alpha_R^{(n_\ell)}))\}$ , and  $I_{\alpha, \ell}$  is the domain of the PDF  $p(\alpha_R^{(n_\ell)})$  in (16).

#### IV. SIMULATION CHANNEL MODEL

In this section, we propose a low complexity SOC channel simulation model to simulate the propagation characteristics in underwater acoustic channels. It is assumed that the scattering environments are anisotropic. Based on the deterministic channel theory, we assume that the number of scatterers  $N_1$  and  $N_2$  tend to be infinite. In this case, the time-varying spatial correlation function of the proposed simulation channel model can be expressed as [22]

$$\begin{aligned} \hat{\rho}_{HH}(\tau, \nu') &= \frac{K}{1 + K} e^{j2\pi(f_0\tau - \tau'_0\nu')} \\ &+ \frac{1}{1 + K} \times \sum_{n_\ell=1}^{N_\ell} c_{n_\ell}^2 e^{j2\pi[f_{n_\ell}\tau - \nu'\tau'_{n_\ell}]} \end{aligned} \quad (26)$$

where  $f_{n_\ell} = \frac{\nu_R}{c_s} \cos(\alpha_R^{(n_\ell)} - \eta_\nu)$ ,  $c_{n_\ell}$  represents the channel complex gain of the  $\ell$ -th propagation path, which can be

expressed as

$$c_{n_\ell} = \frac{A_s(D_{n_\ell})A_a(D_{n_\ell})}{\sqrt{2 \sum_{n_\ell=1}^{N_\ell} A_s^2(D_{n_\ell})A_a^2(D_{n_\ell})}} \quad (27)$$

To parameterize the simulation model, we first provide a parameter calculation method in the following. Then, we compare the system performance of the proposed underwater acoustic channel model based on the MESS method with that of the model based on the traditional Lp-norm method.

#### A. MESS

In this subsection, we adopt the MESS method to calculate the model parameters of the simulation channel. Let us assume that the scatterers are distributed on the surface and bottom of the sea. In this case, when the position of the origin of the Cartesian coordinate and the position of the scatterer  $s^{(n_\ell)}$  are fixed, we can determine the AoA  $\alpha_R^{(n_\ell)}$ . Therefore, the coordinates of the scatterer  $s^{(n_\ell)}$  can be expressed as

$$x_{\ell, n} = \Delta x_\ell(n - 1) + \delta_{x_\ell}, \quad n_\ell = 1, 2, \dots, N_\ell, \ell = 1, 2 \quad (28)$$

$$y_\ell = \begin{cases} D_{T, s}, & \ell = 1 \\ -D_{T, b}, & \ell = 2 \end{cases} \quad (29)$$

where  $\Delta x_\ell = D/N_\ell$ , which can be used to determine the position of the first scatterer on the surface or the bottom of the sea. In the following, we adopt the error function to obtain the optimal solution of the  $\delta_{x_\ell}$ , i.e.,

$$\begin{aligned} \mathbb{E}(\delta_{x_\ell}) &= \frac{1}{v'_{max} \tau_{max}} \\ &\times \int_0^{v'_{max}} \int_0^{\tau_{max}} |\rho_{HH}(\tau, \nu') - \hat{\rho}_{HH}(\tau, \nu')|^2 d\tau d\nu' \end{aligned} \quad (30)$$

Observe from the simulation results of the error function  $\mathbb{E}(\delta_{x_\ell})$  in fig. 2, when we set  $\delta_{x_\ell} = \delta_{x_\ell}^{opt} = \Delta x_1/2$ , we are able to obtain the optimal solutions  $x_{n_\ell}$ , which can be calculated as

$$\delta_{x_\ell}^{opt} = \frac{D_\ell}{N_\ell} \left(n_\ell - \frac{1}{2}\right) \quad (31)$$

It is worth mentioning that the optimal solution  $\delta_{x_\ell}$  is related to the propagation path length between the Tx and MR in the proposed model.

#### B. LP-NORM METHOD

In this subsection, we adopt the Lp-norm method to calculate the model parameters of the simulation channel. In general, we introduce the error function to describe the channel model parameterization, which can be expressed as [19]

$$\begin{aligned} \mathbb{E}(\delta_{x_\ell}) &= \left[ \frac{1}{v'_{max} \tau_{max}} \right. \\ &\times \left. \int_0^{v'_{max}} \int_0^{\tau_{max}} |\rho_{HH}(\tau, \nu') - \hat{\rho}_{HH}(\tau, \nu')|^p d\tau d\nu' \right]^{\frac{1}{p}} \end{aligned} \quad (32)$$

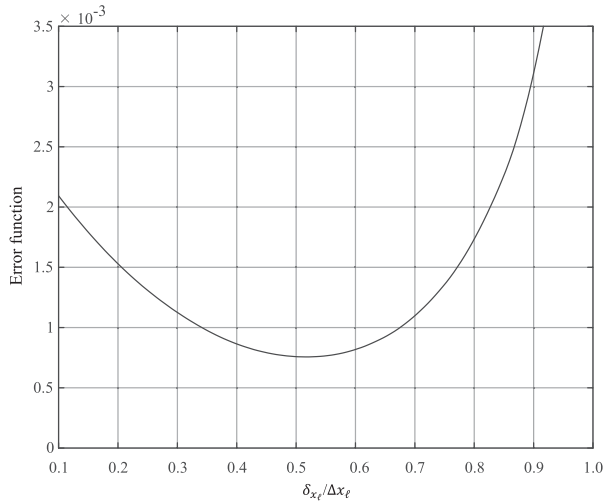


**FIGURE 2.** The error function  $E(\delta_{x_\ell})$  for the optimum value of the  $\delta_{x_\ell}$  when  $N_1 = N_2 = 13$ .

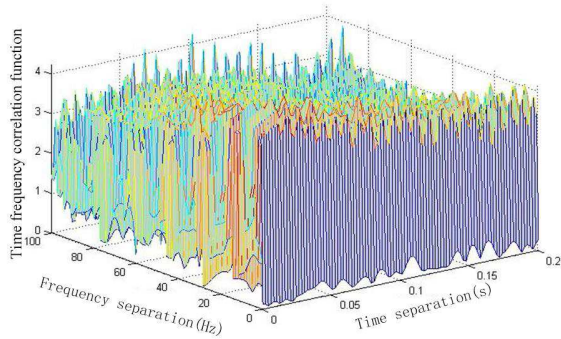


**FIGURE 3.** The spatial correlation of the proposed simulation model with the MESS method when  $N_1 = 80$  and  $N_2 = 79$ .

By minimizing  $\mathbb{E}(\delta_{x_\ell})$  with numerical optimal technologies, we are able to obtain a set of optimal solutions of the AoAs  $\{\alpha_{n_\ell}^{opt}\}$ .

### V. NUMERICAL RESULTS AND DISCUSSIONS

In this section, the statistical channel properties of the proposed model are investigated. To highlight the importance of the underwater scattering environments on the propagation characteristics, we mainly investigate the spatial correlation of two different NLoS propagation paths, that is,  $K = 0$ . Unless otherwise specified, all the channel related parameters used in this section are listed as follows:  $D_{T,s} = 60$  m,  $D_{T,b} = 40$  m,  $D_{R,s} = 20$  m,  $D_{R,b} = 80$  m,  $D = 0.5$  km,  $f_0 = 10$  kHz,  $v_R = 9$  m/s, and  $\eta_v = 0$ .

By using (30), the spatial correlations of two different NLoS propagation paths in the proposed model with the MESS method are investigated in Figs. 3 and 4. It can be observed that the spatial correlation gradually decrease as the time separation increases from 0 s to 0.2 s. It also can be noted that the spatial correlation decreases as the frequency separation increases. Furthermore, when the number of the

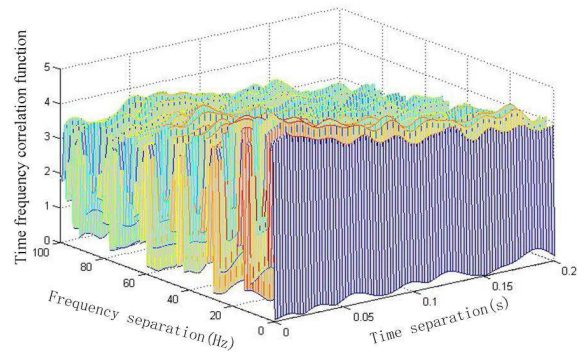


**FIGURE 4.** The spatial correlation of the proposed simulation model with the MESS method when  $N_1 = 150$  and  $N_2 = 149$ .

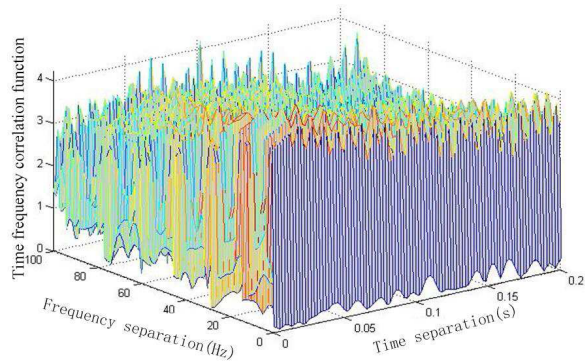


**FIGURE 5.** The spatial correlation of the proposed simulation model with the Lp-norm method when  $N_1 = 80$  and  $N_2 = 79$ .

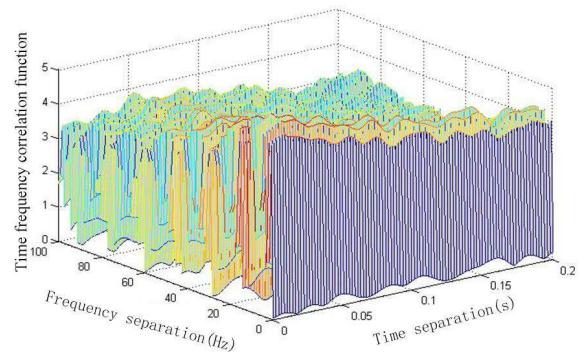


**FIGURE 6.** The spatial correlation of the proposed simulation model with the Lp-norm method when  $N_1 = 150$  and  $N_2 = 149$ .

scatterers on the surface of the sea increases from  $N_1 = 80$  to  $N_1 = 150$ , and the number of the scatterers on the bottom of the sea increases from  $N_2 = 79$  to  $N_2 = 149$ , the spatial correlations with the MESS method vary more consistent. Note that when we set  $\tau_{max} = 0.2$  s and  $v'_{max} = 100$  Hz, the integral value of the square error can be calculated as  $2.19 \times 10^{-4}$ . The above observations fit the the results in [18] very well, which demonstrate the accuracy of the proposed results.

By using (32), the spatial correlations of two different NLoS propagation paths in the proposed model with the

Lp-norm method are investigated in Figs. 5 and 6. It is obvious that when the number of scatterers increases tends to be infinite, the spatial correlation of the simulation model is closer to the reference model. Similar as before, the spatial correlation decreases slowly as the time separation or the frequency separation increases. Note that when we set  $\tau_{max} = 0.2$  s and  $\nu' = 100$  Hz, the integral value of the square error with the MESS method is  $6.24 \times 10^{-5}$ ; however, for the Lp-norm method, the square error integral is  $E(\delta_{x_t}) = 6.07 \times 10^{-5}$ . Furthermore, when there exist significant increase on the numbers of the scatterers (i.e.,  $N_1$  and  $N_2$ ), the performance of the communication systems with the MESS and Lp-norm methods improve to a certain extent; however, the error decreases gradually. In addition, we notice that the design of the performance improvement of the proposed model with the MESS method is particularly significant.

## VI. CONCLUSION

In this paper, we have provided a geometric channel model for underwater acoustic communication environments. Based on the derived PDFs of the AoD and AoA statistics, the spatial correlation functions of two different propagation paths have been investigated. The numerical results have demonstrated that when the numbers of the scatterers on the surface and bottom of the sea increase, the spatial correlations with the MESS method vary more consistent. It has also been shown that the spatial correlation decreases gradually as the time separation or the frequency separation increases. Based on the above observations, the proposed underwater acoustic channel model with the MESS method has the ability to provide the system with better performance than the other methods. The proposed design method in this paper reduces the complexity of the system design and simulation, which extends the research of the channel modeling in underwater acoustic communication environments.

## REFERENCES

- [1] A. Baptista, B. Howe, J. Freire, D. Maier, and C. T. Silva, "Scientific exploration in the era of ocean observatories," *Comput. Sci. Eng.*, vol. 10, no. 3, pp. 53–58, May 2008.
- [2] B. J. Davis, P. T. Gough, and B. R. Hunt, "Modeling surface multipath effects in synthetic aperture sonar," *IEEE J. Ocean. Eng.*, vol. 34, no. 3, pp. 239–249, Jul. 2009.
- [3] V. Kebkal, K. Kebkal, and O. Kebkal, "Experiments with network coding in dynamic underwater acoustic channel," in *Proc. Underwater Commun. Netw. (UComms)*, Sep. 2014, pp. 1–4.
- [4] M. Patzold, *Mobile Radio Channels*, 2nd ed. West Sussex, U.K.: Wiley, 2012.
- [5] M. Stojanovic and J. Preisig, "Underwater acoustic communication channels: Propagation models and statistical characterization," *IEEE Commun. Mag.*, vol. 47, no. 1, pp. 84–89, Jan. 2009.
- [6] F. Jia, E. Cheng, and F. Yuan, "The study on time-variant characteristics of under water acoustic channels," in *Proc. Int. Conf. Syst. Inf. (ICSAI)*, May 2012, pp. 1650–1654.
- [7] H. Jiang, Z. Zhang, J. Dang, and L. Wu, "Analysis of geometric multi-bounced virtual scattering channel model for dense urban street environments," *IEEE Trans. Veh. Technol.*, vol. 66, no. 3, pp. 1903–1912, Mar. 2017.
- [8] H. Jiang, Z. Zhang, and G. Gui, "A novel estimated wideband geometry-based vehicle-to-vehicle channel model using an AoD and AoA estimation algorithm," *IEEE Access*, vol. 7, pp. 35124–35131, 2019.
- [9] A. Abdi and H. Guo, "Signal correlation modeling in acoustic vector sensor arrays," *IEEE Trans. Signal Process.*, vol. 57, no. 3, pp. 892–903, Mar. 2009.
- [10] A. G. Zajic, "Statistical modeling of underwater wireless channels," in *Proc. IEEE Global Telecommun. Conf. (GLOBECOM)*, Dec. 2010, pp. 1–5.
- [11] A. G. Zajic, "Statistical modeling of MIMO mobile-to-mobile underwater channels," *IEEE Trans. Veh. Technol.*, vol. 60, no. 4, pp. 1337–1351, May 2011.
- [12] M. Naderi, A. G. Zajic, and M. Pätzold, "A nonisovelocity geometry-based underwater acoustic channel model," *IEEE Trans. Veh. Technol.*, vol. 67, no. 4, pp. 2864–2879, Apr. 2018.
- [13] A. Wang, B. Li, and Y. Zhang, "Underwater acoustic channels characterization for underwater cognitive acoustic networks," in *Proc. Int. Conf. Intell. Transp., Big Data Smart City (ICITBS)*, Jan. 2018, pp. 223–226.
- [14] T. C. Yang, "A study of spatial processing gain in underwater acoustic communications," *IEEE J. Ocean. Eng.*, vol. 32, no. 3, pp. 689–709, Jul. 2007.
- [15] H. Jiang, Z. Zhang, and G. Gui, "Three-dimensional non-stationary wide-band geometry-based UAV channel model for A2G communication environments," *IEEE Access*, vol. 7, pp. 26116–26122, 2019.
- [16] H. Huang, J. Yang, H. Huang, Y. Song, and G. Gui, "Deep learning for super-resolution channel estimation and doa estimation based massive MIMO system," *IEEE Trans. Veh. Technol.*, vol. 67, no. 9, pp. 8549–8560, Sep. 2018.
- [17] B. Liu, G. Gui, S. Matsushita, and L. Xu, "Dimension-reduced direction-of-arrival estimation based on  $\ell_{2,1}$ -norm penalty," *IEEE Access*, vol. 6, pp. 44433–44444, 2018.
- [18] P. Qarabaqi and M. Stojanovic, "Statistical characterization and computationally efficient modeling of a class of underwater acoustic communication channels," *IEEE J. Ocean. Eng.*, vol. 38, no. 4, pp. 701–717, Oct. 2013.
- [19] M. Patzold, *Mobile Fading Channels*, 2nd ed. Chichester, U.K.: Wiley, 2011, pp. 23–56.
- [20] H. Jiang, Z. Zhang, L. Wu, and J. Dang, "A non-stationary geometry-based scattering vehicle-to-vehicle MIMO channel model," *IEEE Commun. Lett.*, vol. 22, no. 7, pp. 1510–1513, Jul. 2018.
- [21] H. Jiang, Z. Zhang, J. Dang, and L. Wu, "A novel 3-D massive MIMO channel model for vehicle-to-vehicle communication environments," *IEEE Trans. Commun.*, vol. 66, no. 1, pp. 79–90, Jan. 2018.
- [22] M. Patzold, C.-X. Wang, and B. O. Hogstad, "Two new sum-of-sinusoids-based methods for the efficient generation of multiple uncorrelated Rayleigh fading waveforms," *IEEE Trans. Wireless Commun.*, vol. 8, no. 6, pp. 3122–3131, Jun. 2009.

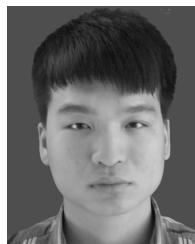


**JIE ZHOU** is a Professor with the Department of Electronic and Electrical Engineering, Nanjing University of Information Science and Technology, China and Electronic Engineering, Niigata University, Japan. His current research interests include mobile communication theory and applications, radio access networks, and wireless sensor networks.



**HAO JIANG** (M'19) received the B.S. and M.S. degrees in electrical and information engineering from the Nanjing University of Information Science and Technology, Nanjing, China, in 2012 and 2015, respectively, and the Ph.D. degree from the National Mobile Communications Research Laboratory, Southeast University, Nanjing, China, in 2019. From 2017 to 2018, he was a Visiting Student with the Department of Electrical Engineering, Columbia University, New York, NY, USA.

Since 2019, he has been a Professor with the School of Information Science and Engineering, Nanjing University of Information Science and Technology. His current research interests include general area of vehicle-to-vehicle communications, massive multiple-input and multiple-output channel modeling, signal processing, communications, machine learning, and AI-driven technologies.



**PENG WU** is with the Department of Electronic and Electrical Engineering, Nanjing University of Information Science and Technology, China. His current research interests include mobile communication theory and applications, and radio access networks.



**QIAN CHEN** is with the Department of Electronic and Electrical Engineering, Nanjing University of Information Science and Technology, China. Her main research interests include mobile communication theory and applications, and radio access networks.

...